УДК: 577.35+611.018.61.+547.857.7

D.O. DRYN,[1] A. V. GRYSHCHENKO,[2] T. B. BOLTON,[3] M. X. ZHU,[4] AND A. V. ZHOLOS[1,2]

SPECIES-RELATED DIFFERENCES IN THE PROPERTIES OF RECEPTOR-OPERATED TRPC4 CHANNELS IN INTESTINAL MYOCYTES OF RODENTS

Received December 20, 2014

TRPC4 proteins form receptor-operated cation channels that are activated in synergy by M_2 and M_3 acetylcholine (ACh) receptors coupled to $G_{q/11}$ and $G_{i/o}$ proteins, respectively. These channels are widely expressed in the brain and smooth muscles where they perform a number of important functions, including control of GABA release from the dendrites and cholinergic excitation of smooth muscles. The biophysical properties of TRPC4 currents directly activated by GTPγS in mouse cells remain mostly unknown. We, thus, aimed to investigate these channels in mouse ileal myocytes where a prominent TRPC4-mediated cation current termed mI_{CAT} is observed, and to compare the behavior of this current with that of the better studied mI_{CAT} in guinea-pig myocytes. Although the respective cation current responses to carbachol (CCh) at –50 mV (i.e., at the value close to the normal resting potential in these cells) were highly similar, mI_{CAT} in the mouse lacked the permissive action of intracellular Ca^{2+} on channel opening. The slope factor of the muscarinic cation conductance, which is a defining property of voltage-dependent behavior, was identical in both species. There were differences in the potential at which the current peaked at negative potentials, but not in the maximal current densities. Major differences were found in the kinetics of mI_{CAT} voltage-dependent relaxations, which were much faster in the mouse. The above rodent species employ two different strategies for the open probability increase by activated G-proteins; the mean open time was shorter in the mouse compared to that in the guinea-pig (15.1 ± 5.2 msec, n = 8, vs. 80.0 ± ± 19.7 msec, n = 9; $P < 0.01$). Correspondingly, the instantaneous frequency of channel opening was much higher in the mouse (154.1 ± 18.8 sec^{-1} vs. 70.2 ± 7.3 sec^{-1} in the guinea-pig; $P < 0.001$). These functional differences are based on the differences found in the corresponding TRPC4 amino acid sequences of the two rodent species, which are mainly clustered in the cytosolic C-terminus of TRPC4 protein.

Keywords: muscarinic receptors, receptor-operated cation channels, TRPC4, G-proteins, species-related differences

INTRODUCTION

G protein-coupled muscarinic acetylcholine receptors (mAChRs) are widely expressed in various visceral smooth muscles, in particular, in those of the gastrointestinal tract, respiratory tract, and genitourinary system. These receptors are predominantly represented by the M_2 and M_3 subtypes typically expressed at a ratio of 4:1–5:1 [1]. Such receptors mediate neurogenic visceral smooth muscle contractions. In this case, acetylcholine is the primary excitatory neurotransmitter that causes membrane depolarization, generation of an action potential (AP), and intense Ca^{2+} influx (mainly via L-type calcium channels), thus causing myocyte contraction. Muscarinic effects on smooth muscle ion channels are very complicate (these effects involve multiple channel types [2]). Nonetheless, activation of cation channels, which generates an inward muscarinic cation current termed mI_{CAT}, has been recognized as the key event in the cholinergic excitation-contraction coupling in gastrointestinal and other smooth muscles [2–7].

A number of classical works on the ion nature of the cholinergic control of gastrointestinal smooth

[1] Educational and Scientific Center "Institute of Biology," Taras Shevchenko National University, Kyiv, Ukraine
[2] Bogomoletz Institute of Physiology, National Academy of Sciences of Ukraine, Kyiv, Ukraine
[3] St. George's University of London, London, Great Britain
[4] University of Texas, Health Science Center at Houston, Houston, Texas, USA
Address correspondence to:
A. V. Zholos a.zholos@univ.net.ua

muscles have been carried out using guinea-pig tissues (mainly *ileum* and *taenia coli*) [8]. With the advent of the patch-clamp techniques, the ileum and stomach of the guinea-pig became tissues of choice for detailed characterization of biophysical and pharmacological properties of mI_{CAT}, as well as of signal transduction pathways linking mAChRs to cation channels [3–6, 9]. These studies have provided a wealth of information on the activation mechanisms of mI_{CAT} (summarized in Fig. 1A). Briefly, three crucial events resulting in the muscarinic cation channel opening are the following: (i) $G_{i/o}$ activation by the M_2 receptor subtype that primarily controls channel opening [10, 11], (ii) subsequent activation of M_3 receptors coupled to the $G_{q/11}$/PLC/$InsP_3$ (phospholipase C/inositol trisphosphate) system, which somehow enables and potentiates channel opening [10], and (iii) a rise in the intracellular free Ca^{2+} concentration ($[Ca^{2+}]_i$). Some minimal $[Ca^{2+}]_i$ level is critically required for mI_{CAT} (a permissive effect); in addition, a rise in the $[Ca^{2+}]_i$ (a secondary effect with respect to membrane depolarization) strongly potentiates and then inhibits channel activity [12–15]. Moreover, mI_{CAT} displays a characteristic current-voltage (I–V) relationship; the latter is doubly rectifying around the reversal potential and U-shaped at negative potentials [16–18]. In addition, its voltage dependence is dynamically regulated by G-protein activation [19].

More recently, we have validated a mouse model for the study of mI_{CAT} [20]; this seemed to be very useful in view of new opportunities for more accurate identification of the channel gating mechanisms

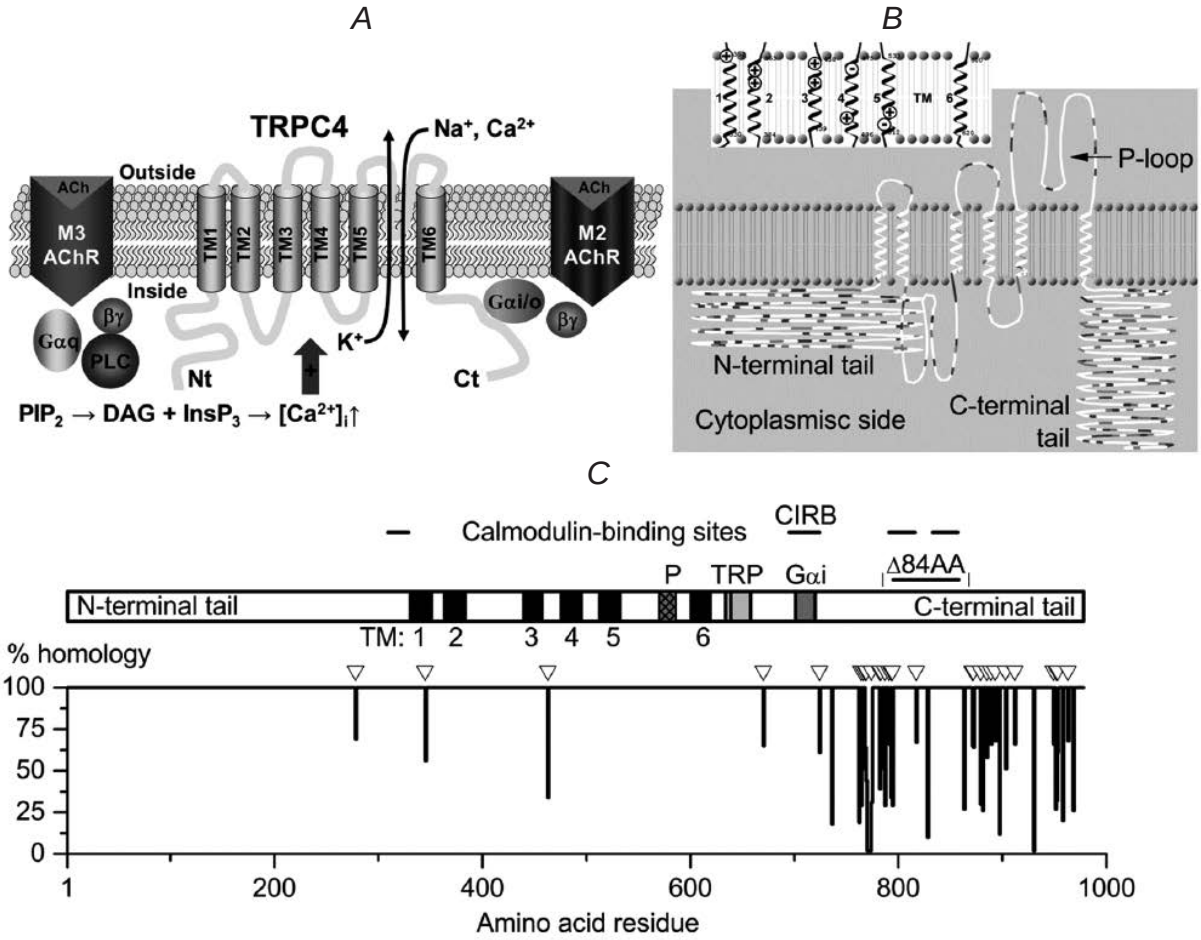

F i g. 1. Structural relations in guinea-pig and mouse TRPC4 proteins. A) General topology of the TRPC4 channel and the main signalling events coupling M_2 and M_3 muscarinic receptor activation and the TRPC4 opening. B) 2D TRPC4 structure modeled with TMRPres2D [29]; transmembrane domains of the channel are shown in the inset depicting several positively and negatively charged amino acid residues in the TM1-TM6 segments. C) Positions of several structural domains (1) and CLUSTALX 2.1 [31] column scores for the aligned amino acid sequences of mouse and guinea-pig TRPC4s (2); UniProtKB accession numbers: *Mus musculus*, Q9QUQ5; *Cavia porcellus*, B8Q884. Positions of similar amino acid residues are indicated by open triangles.

Р и с. 1 . Структурні взаємовідносини у білків TRPC4 морської свинки та миші.

in myocytes of genetically modified mice lacking certain receptors, G proteins, or channel proteins. Such experiments allowed us to obtain detailed characteristics of the three distinct muscarinic signalling pathways for cation channel activation in murine gut smooth muscle cells lacking M_2 receptors, M_3 receptors, or both [21]. These studies also revealed the molecular counterparts of mI_{CAT}; this current predominantly produced via TRPC4 and, to a lesser extent, via TRPC6 channel proteins [22, 23]. Channel identification, in turn, opened possibilities to develop additional molecular approaches using TRPC4 proteins heterologously expressed in HEK293 cells. This way, several $G\alpha_i$ subunits (most importantly, $G\alpha_{i2}$) have been identified as direct activators of TRPC4, which act via binding to a domain in the C-terminus of the channel [24] (Fig. 1A). Hydrolysis of phosphoinositol 4,5-bisphosphate (PIP_2) by PLC (an M_3 effect) is a prerequisite for mI_{CAT} generation, as at least the full-length TRPC4α isoform is inhibited by PIP_2 [25]. The complex roles of intracellular calcium in the mI_{CAT} regulation may now also be better understood considering that TRPC channels have multiple calmodulin (CaM)-binding domains [26].

Considering the ever-growing list of sequenced animal genomes and wide interest in receptor-operated and sensory channels comprising the large ion channel superfamily of TRPs [27], it is now timely to address the structure/function relations in these channels based on their species-related differences within the Rodentia order. Such studies will undoubtedly provide not only novel insights into the role of certain naturally occurring structural differences, but also can inform us of the most appropriate animal models for translational research. Here, we analyzed structural differences in guinea-pig and murine TRPC4 proteins. It is shown by comparing corresponding native mI_{CAT} currents in ileal myocytes recorded under identical conditions; although these channels share some major voltage-dependent properties, there are considerable differences in their intracellular calcium dependence, and these channel structures employ different strategies to increase the channel open probability by activated G-proteins.

METHODS

Cell isolation. Adult (3 months) Balb/C male mice weighing 30-35 g and male guinea pigs (300–400 g) were euthanized by vertebral dislocation at the cervical level followed by immediate exsanguination. The longitudinal muscle layer from the small intestine (ileum) was quickly dissected and placed into modified Krebs solution of the following composition (mM): NaCl, 120; KCl, 6.0; $CaCl_2$, 2.5; $MgCl_2$, 1.2; glucose, 12, and HEPES, 10 (pH adjusted to 7.4 with NaOH). Muscle strips were then kept for 3–5 min in a Ca^{2+}, Mg^{2+}-free solution (NaCl, 120; KCl, 6.0; glucose, 12, and HEPES, 10; pH 7.4 adjusted with NaOH) where they were cut into small (1–3 mm) pieces. For cell dispersion, those were treated with collagenase type 1A (1.0 mg/ml), trypsin inhibitor (1.0 mg/ml), and bovine serum albumin (1.0 mg/ml) at 36.5°C for 17–18 min (mouse) or 25–28 min (guinea-pig); this was followed by trituration until a cloudy cell suspension was obtained.

Patch-clamp recordings. Transmembrane currents were recorded in the whole-cell or outside-out configurations of the patch-clamp techniques using an Axopatch 200B voltage-clamp amplifier and Digidata 1322A + pClamp 8 software (Molecular Devices, USA). Patch pipettes, made from borosilicate glass (outer/inner diameters, 1.5/0.86 mm, Harvard Apparatus, USA) using a P-97 micropipette puller (Sutter Instrument Co, USA), had a resistance of 3–5 MΩ when filled with the intracellular solution. Transmembrane currents were filtered at 2 kHz and sampled at 10^4 sec^{-1}. In whole-cell measurements, the series resistance was compensated for by ~ 65%, and the holding potential was –40 mV. The steady-state current-voltage relationships (I–V curves) were measured using slow-voltage ramps (6-sec-long duration from 80 mV to –120 mV applied with 30-sec intervals). Muscarinic cation channel currents were isolated using symmetrical Cs^+ solutions. The external solution contained (mM): CsCl, 120; glucose, 12, and HEPES 10; pH adjusted to 7.4 with CsOH (total Cs^+ 125 mM), while the pipette solution contained CsCl, 80; MgATP, 1.0; GTP, 1.0 (replaced by 200 μM GTPγS in some experiments); creatine, 5.0; glucose, 5.0; BAPTA, 10; HEPES, 10, and $CaCl_2$, 4.6 (or, in some experiments, without added Ca^{2+}); pH was set to 7.4 by adding CsOH (total Cs^+ 125 mM). The mI_{CAT} was activated by applying a stable muscarinic receptor agonist, CCh, at a submaximally effective concentration (50 μM) [10] or by intracellular infusion of guanosine 5′-O-(3-thiotriphosphate) (GTPγS) by adding 200 μM of the latter to the pipette solution (this maneuver activates G-proteins directly, i.e., bypassing the muscarinic receptors [28]). All experiments were carried out at room temperature (22–25°C).

Materials. Most chemicals and reagents, including collagenase 1A, bovine serum albumin (BSA), trypsin inhibitor, carbamylcholine chloride (CCh), CsCl , BAPTA, GTPγS (tetralithium salt), creatine, HEPES, ATP (magnesium salt), etc., were obtained from Sigma-Aldrich Chemical Co. (USA).

Bioinformatics analysis. Visualization of the two-dimensional TRPC4 structure was performed using the "TransMembrane protein Re-Presentation in 2 Dimensions" tool (TMRPres2D) [29]. Analysis of amino acid sequences found in the UniProtKB database was done using standard tools, such as the Basic Local Alignment Search Tool (BLAST), Clustal Omega alignment [30], and CLUSTALX 2.1 [31].

Data analysis. Data were analyzed, fitted, and plotted using Clampfit 8 and/or Origin 2016 software (OriginLab Corp., USA). All numerical values are expressed below as means ± s.e.m; *n* represents the number of cells or membrane patches tested. The Student's *t*-test was used for statistical comparison, and intergroup differences were accepted as statistically significant at two-tail $P \leq 0.05$.

RESULTS AND DISCUSSION

Bioinformatics analysis. The ever-growing number of sequenced animal genomes now allows researchers, by amino acid sequence alignment, to evaluate the evolutionary and structure-function relations between different proteins. This analysis showed that TRPC4 homology in different species varied from 62 to 100%. Here, we focused on the analysis of TRPC4 structural relatedness in two rodent species only, the guinea pig and the mouse, in which TRPC4-mediated mI_{CAT} has been most extensively characterized up to the single-channel level [20, 21, 28]. Figure 1B shows the 2D structural diagram of TRPC4. It is notable that charged amino acids (AAs) are lacking in its transmembrane (TM) segments, which is common for all other TRP subtypes. It is, thus, puzzling that several TRPs (including TRPC4s and highly related receptor-operated TRPC5s, as well as several temperature-sensitive TRPV1s, TRPA1s, and TRPM8s) show prominent voltage-dependent gating [32].

Several structural features of TRPC4 already described in the Introduction (see also a recent comprehensive review [33]) are illustrated in Fig. 1C. This receptor included six TM segments, a re-entry pore-forming sequence (or P-loop, P), and a highly conserved TRP domain containing the initial TRP box "signature" (EWKFAR), a Gαi-binding site [24], and four calmodulin-binding sites, one of which (CIRB) also binds the $InsP_3$ receptor [34]. The PIP_2-binding site is not well defined, but a shorter TRPC4β variant, lacking the indicated Δ84 AA stretch, is not inhibited by PIP_2 [25]. While guinea-pig and mouse TRPC4s show an overall 95.6% identity (among 977 AAs in the guinea-pig and 974 AAs in the mouse, 935 AAs are found in identical positions, and 29 AAs are in similar positions), it is notable that 93% of all AA differences are clustered in its distal C-terminal tail, while those occurring in the N-terminus and within the TM region are all similar substitutions (open triangles in Fig. 1C). Thus, one can envisage that some major properties of mouse and guinea-pig mI_{CAT} may be highly similar, especially considering the highly conserved channel core of the TM1-TM6 region), while there may also be differences in current regulation attributed to the structural differences in the C-terminus.

Indeed, we have previously extensively studied the voltage dependence of mI_{CAT} in guinea-pig ileal myocytes [19, 28, 35] and, to a lesser extent, in mouse ileal myocytes [20], including the underlying single-channel behavior, and noted relative similarities in the single channel conductance (57 and 70 pS, respectively) and Boltzmann factor (k) describing the slope of the channel voltage dependence. At the same time, the potential of half-maximal activation ($V_{1/2}$) and channel open probability (Po) seemed to be sufficiently dissimilar in these two species. Here, we provide a direct comparison of I-V curves measured under identical conditions and for the first-time address of the intracellular Ca^{2+} requirement of channel activation. We also introduce a new model of GTPγS-induced currents in mouse myocytes for systematic analysis of the voltage-dependent relaxation kinetics, expecting to identify some additional species-dependent differences.

Analysis of CCh-induced mI_{CAT}. Figure 2A shows that the kinetics of mI_{CAT} induced by the receptor agonist CCh were partically indistinguishable in the two examined rodent species. On average, the rise time from 10 to 90% of the maximal current amplitude (t_{10-90}) was 10.47 ± 0.70 sec in guinea-pig myocytes (n = 17; ranged from 5.52 to 14.35 sec) and 10.95 ± ± 1.10 sec in mouse cells (n = 12; ranged from 5.90 to 16.52 sec).

Inoue and Isenberg [12] first noted the permissive action of $[Ca^{2+}]_i$ on mI_{CAT} in guinea-pig ileal myocytes. In the mentioned experiments, 40 mM EGTA was used to bring $[Ca^{2+}]_i$ below 1 nM, and this procedure nearly

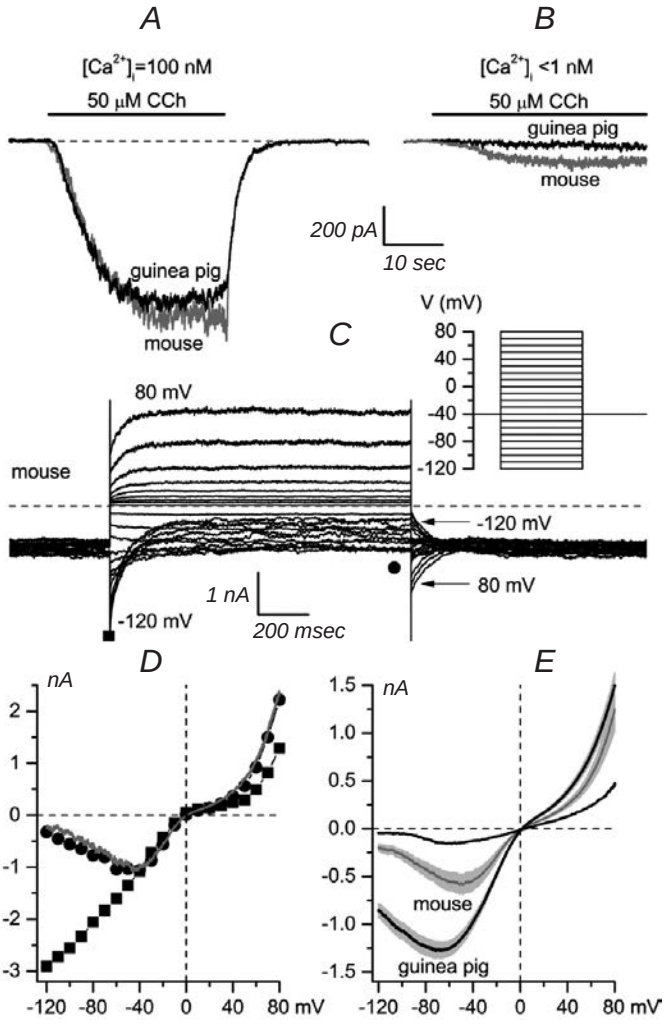

F i g. 2. Comparison of carbachol (CCh)-induced mI_{CAT} in guinea-pig and mouse ileal myocytes. A and B) Superimposed cation current responses to 50 μM CCh application in the cells held at –50 mV (guinea-pig, black lines; mouse, gray lines) recorded with intracellular Ca^{2+} strongly buffered at 100 nM (A) or at <1 nM $[Ca^{2+}]_i$ (B, 10 mM BAPTA, no added Ca^{2+} in the pipette solution). C) Superimposed mI_{CAT} traces recorded in a mouse ileal myocyte in the presence of 50 μM CCh in the external solution at different test potentials ranging from –120 to 80 mV using the voltage protocol shown in the inset. D) Corresponding I-V relationships of the peak (squares) and steady-state (circles) currents during the voltage steps, as shown by the respective symbols in C; the I-V curve measured in the same cell by applying a slow 6-sec-long voltage ramp from 80 to –120 mV is also shown (gray line). E) Averaged I-V relationships (means ± s.e.m.) measured by voltage ramps in guinea-pig (black line; $n = 32$) and mouse (gray line; $n = 17$) ileal myocytes at the peak response to CCh (50 μM) application; for comparison, dashed line shows the I-V curve measured in a mouse myocyte with $[Ca^{2+}]_i < 1$ nM.

Р и с. 2. Порівняння індукованих аплікаціями карбахолу струмів mI_{CAT} у міоцитах ілеуму морської свинки та миші.

abolished mI_{CAT}. Using 10 mM BAPTA in the pipette, we found that, without adding Ca^{2+} to "clamp" $[Ca^{2+}]_i$ at 100 nM as normally, guinea-pig mI_{CAT} in response to 50 μM CCh application was negligible (–4.3 ± 1.9 pA at –50 mV, $n = 3$), but mouse mI_{CAT} under identical conditions was well-measurable (–137.6 ± 25.2 pA, $n = 5$). This was about 25% of the normal response at the same potential with $[Ca^{2+}]_i$ =100 nM (compare to Fig. 2E). Two other, not yet molecularly identified, cation channels with the unitary conductances of 10–17 and 130–140 pS make a relatively small contribution to mI_{CAT} [20, 21, 28]. Thus, we also verified that the small mI_{CAT} recorded with $[Ca^{2+}]_i$ below 1 nM has a voltage dependence typical of the major TRPC4-mediated component of mI_{CAT} (Fig. 2E, dashed line). Thus, we can convincingly conclude that, an important permissive effect of intracellular Ca^{2+} present in guinea-pig TRPC4 is lacking in mouse TRPC4. The molecular basis of the Ca^{2+} dependence of TRPC4 is not yet known, but it is likely that the four CaM binding domains (Fig. 1C) play a role. If so, it is interesting to note that three AA differences are present in one of the two CaM domains in the C-terminus, in which an adjacent His-Phe segment in the guinea-pig receptor is replaced by Asn-Leu in the mouse one. It would be, thus, interesting to compare the intracellular Ca^{2+} dependence of TRPC4α and TRPC4β isoforms, as both isoforms are naturally expressed in the mouse intestine [25], but this CaM-binding domain is absent in the shorter TRPC4β variant.

The voltage dependence of mouse mI_{CAT} was further examined in detail by applying voltage steps at maximal current activation by CCh (Fig. 2C) and by plotting both instantaneous and steady-state I-V curves (Fig. 2D). We also verified that an I-V curve closely similar to the latter could be obtained by applying slow (6 sec) voltage ramps (Fig. 2D, gray continuous line). This behavior is now well understood as the intrinsic voltage dependence of mI_{CAT} [16, 18] regulated by G-protein activity [19], while quantitative analysis of mI_{CAT} voltage-dependent relaxations remains lacking. Mean steady-state I-V relations of guinea-pig and mouse mI_{CAT} are compared in Fig. 2E. The $V_{1/2}$ values differed from each other somewhat (–78.3 ± 2.1 mV, $n = 32$ vs. –64.6 ± 4.2 mV, $n = 17$, respectively; $P = 0.002$). At the same time, the Boltzmann slope factor was practically identical (k = –15.9 ± 0.7 mV vs. –16.1 ± ± 0.8 mV). Correspondingly, mI_{CAT} peaked at –70 mV, producing a current density of –23.2 ± 1.7 pA/pF in

the guinea-pig and at –50 mV (–19.2 ± 2.0 pA/pF) in the mouse. Thus, the maximal current densities (P = 0.153), as well as the reversal potentials of these currents (1.9 ± 0.3 mV vs. 1.7 ± 0.4 mV, respectively) were nearly similar in both rodent species.

However, substantial differences were observed in the mI_{CAT} voltage-dependent relaxation kinetics. In the guinea-pig, the deactivation time constant during a voltage step to –120 mV was 178.9 ± 18.3 msec (n = 17) compared to 58.2 ± 4.6 msec (n = 28) in the mouse (P < 0.0001), while the reactivation time constant at –40 mV was 104.6 ± 7.5 msec vs. 84.8 ± ± 5.7 msec, respectively (P < 0.05).

One difficulty in studying CCh-induced currents is muscarinic receptor desensitization. Although it can be alleviated by adding 1 mM GTP to the pipette solution [35], one can notice the drift of the baseline current before voltage steps during the time needed to apply the required series of steps (Fig. 2C). We, thus, introduced a more robust model of GTPγS-induced currents for studying mouse mI_{CAT} in more detail.

Analysis of GTPγS -induced mI_{CAT}. Figure 3A shows a representative example of GTPγS-induced currents in a mouse ileal myocyte recorded with a combination of voltage steps to –120, 80, and –40 mV and a ramp from 80 to –120 mV. This protocol allowed us to examine I-V curves and, simultaneously, the current relaxation kinetics. Following breakthrough at time zero, the current slowly increased and reached its maximum during 3–8 min in different cells. The respective variations probably reflect differences in the rate of GTPγS infusion depending on the access resistance. After achieving the peak response, the I-V curves and current kinetics were examined in more detail by applying voltage steps within the entire range of potentials, from –120 to 80 mV (Fig. 3C). These currents were similar to CCh-induced currents (cf. Fig. 2C), with the advantage that the baseline current remained stable, indicating the negligible desensitization (at least during the time of measurements) under conditions where G-proteins were activated directly, bypassing mAChRs. An analysis similar to the above-described was performed, as illustrated in Fig. 3D, E. When summarizing these results (guinea pig vs. mouse, respectively), the maximal current density was observed at –72.8 mV in the guinea-pig (–28.9 ± 2.1 pA/pF, n = 21) and at –58.5 mV in the mouse (–23.8 ± 2.5 pA/pF, n =

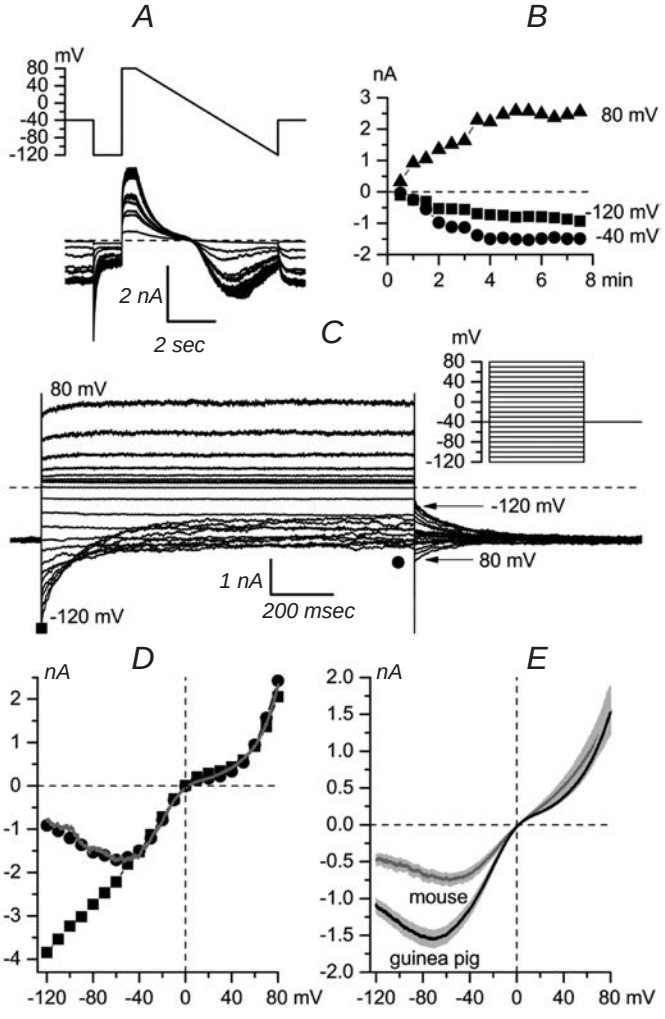

F i g. 3. Comparison of intracellular GTPγS-induced mI_{CAT} in guinea-pig and mouse ileal myocytes. A) Voltage protocol and corresponding superimposed cation current traces recorded in a mouse ileal myocyte during GTPγS infusion via the patch pipette; voltage pulses were applied, and currents were recorded at 30-sec-long intervals beginning shortly (about 20 sec) after breakthrough with 200 μM GTPγS in the pipette solution. B) Time course of current amplitudes measured at –40 mV (holding potential), –120 mV, and 80 mV, as indicated. C) Superimposed mI_{CAT} traces recorded at different test potentials (voltage protocol shown in the inset) in the cell illustrated in A. D) Corresponding I-V relationships of the peak (squares) and steady-state (circles) currents during the voltage steps, as shown by the corresponding symbols in C; the I-V curve measured in the same cell by applying a slow 6-sec-long duration voltage ramp from 80 to –120 mV is shown by gray line. E) Averaged I-V relationships (means ± s.e.m.) measured by voltage ramps in guinea-pig (black line; n = 21) and mouse (gray line; n = 14) ileal myocytes at the peak response to GTPγS (200 μM) intracellular application.

Р и с. 3. Порівняння індукованих внутрішньоклітинною дією ГТФγS струмів mI_{CAT} у міоцитах ілеуму морської свинки та миші.

= 14). The current densities in the two species did not differ significantly from each other (P = 0.13), and their reversal potentials were also nearly similar (1.7 ± ± 0.5 mV vs. 1.2 ± 0.6 mV). The slope factors of the voltage dependence were also practically identical (k = –17.6 ± 1.0 mV vs. –16.0 ± 1.0 mV), but the $V_{1/2}$ values were clearly dissimilar (–82.4 ± 1.7 mV vs. –65.8 ± 4.1 mV; P = 0.0002).

Examination of the voltage-dependent relaxation kinetics of mI_{CAT}. Another important advantage of using GTPγS rather than CCh for mI_{CAT} activation is that the activation phase is well spread in time; this allowed us to repeatedly measure the mI_{CAT} kinetics during gradual build-up of the amount of activated G-proteins; GTPγS binds to their α-subunits spontaneously, slowly, and irreversibly. Typical current traces illustrating alteration of the mI_{CAT} deactivation/reactivation kinetics along with accumulation of activated G-proteins are shown in Fig. 4; panels A and B are for the guinea-pig and mouse, respectively. The traces could be fitted well with single exponential functions, as is shown by the superimposed smooth black lines. Because of substantial cell-to-cell variation of the time required for full activation of mI_{CAT} by GTPγS, averaged data are plotted against the relative time to peak, which in different cells ranged from about 3 to 8 min (Fig. 4C). This analysis revealed that the deactivation rate in the guinea-pig was not only slower compared to that in the mouse but also was more dependent on G-protein activation. Thus, the time constant showed an overall increase to 230% in the mouse, which was in striking contrast to the more than 21-fold change in the guinea-pig (Fig. 4C, left panel). However, the reactivation kinetics showed less dramatic species-related differences (Fig. 4C, right panel). Interestingly, the mean values were not crucially dissimilar shortly after breakthrough (P = 0.131) but became very different at maximal G-protein activation (P = 0.0003). Moreover, the reactivation time constants in both species showed a quite comparable dependence on G-protein activation; an increase in the guinea-pig by 46% vs. 45% in the mouse.

The faster deactivation kinetics of mouse mI_{CAT} is a strong proof for a shorter channel open time. To directly test such differences, the channel activities recorded in outside-out patches excised from cells stimulated by 50 μM CCh and held at –50 mV were compared, as shown in Fig. 4D. Unitary currents were somewhat larger in the mouse (peaks in the amplitude histograms were –3.3 and –2.7 pA, which corresponded

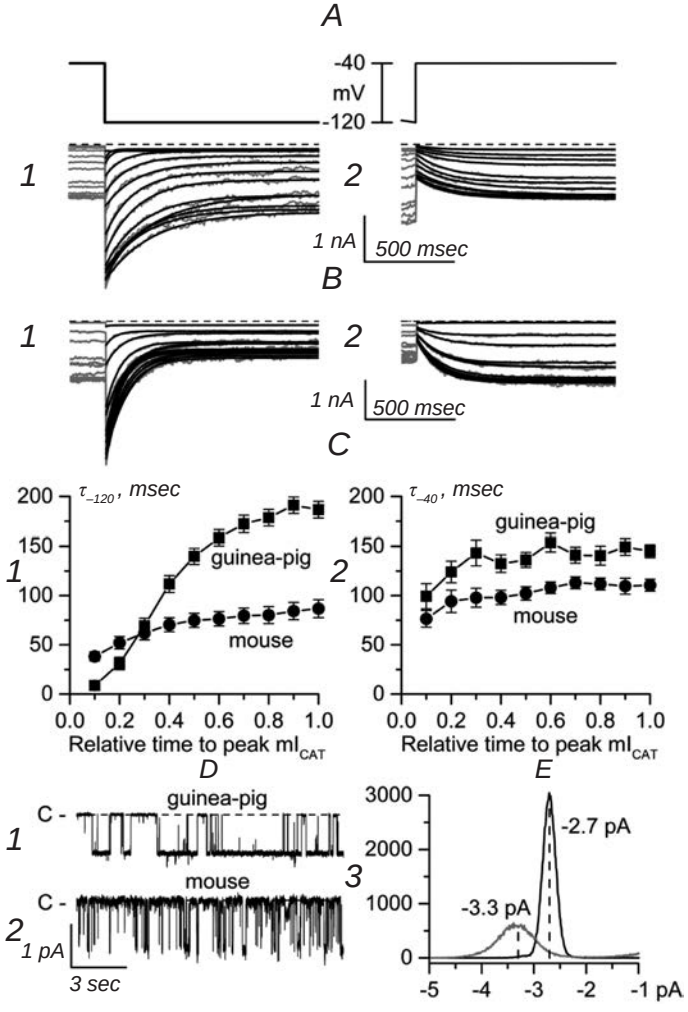

F i g. 4. Comparative analysis of mI_{CAT} voltage-dependent relaxation kinetics in guinea-pig and mouse intestinal myocytes. A and B) During progressive mI_{CAT} activation by intracellular GTPγS infusion, the mI_{CAT} deactivation (1) and reactivation (2) kinetics were examined at 30-sec intervals using the voltage protocol for guinea-pig (A) and mouse (B) ileal myocytes shown in Fig. 3A. Both mI_{CAT} deactivation and reactivation kinetics could be well approximated by a single exponential function, as shown by the superimposed smooth black lines. C) Mean time constants of GTPγS-induced mI_{CAT} deactivation at –120 mV (1) and reactivation at –40 mV (2) in guinea-pig (squares; n = 21) and mouse (circles; n = 25) ileal myocytes. D) For comparison of single-channel gating, outside-out patches isolated from guinea-pig (1) and mouse (2) ileal myocytes were held at –50 mV in the presence of 50 μM CCh; all-point amplitude histograms (bin size 0.1 pA) corresponding to channel openings are shown in panel 3.

Р и с. 4. Порівняльний аналіз кінетики потенціалзалежної релаксації струму mI_{CAT} у міоцитах кишківника морської свинки та миші.

to 66 and 54 pS; cf. the previously reported average values of 69 and 57 pS [20, 28]). In the open state, currents were noticeably "noisier" in mouse myocytes (hence, the peak in the histogram was wider), which may be due to more considerable fluctuations in the channel protein pore. The open probability was also smaller in the mouse (Po = 0.20 ± 0.04, n = 8 vs. 0.58 ± ± 0.04, n = 9; $P < 0.0001$). The channel open probability is determined by the ratio of the mean open time to the closed one. Analysis of the difference in P_o revealed that, indeed, the mean open time was considerably shorter in mouse myocytes compared to that in guinea-pig cells (15.1 ± 5.2 msec, n = 8 vs. 80.0 ± ± 19.7 msec, n = 9; $P < 0.01$). Correspondingly, the instantaneous frequency of channel opening (which is inversely proportional to the duration of channel closings) was much higher in the mouse (154.1 ± ± 18.8 sec^{-1} vs. 70.2 ± 7.3 sec^{-1}; $P < 0.001$).

When summarizing these findings, we should state that several biophysical properties of mI_{CAT} are virtually identical in guinea-pig and mouse myocytes. These characteristics include the shape of the I-V curves and the Boltzmann slope factor, which is the most important parameter for the channel voltage dependence. These findings are not surprising considering the high similarity of the TM1-TM6 region that contains only two altered but similar in their physicochemical properties amino acid residues (Fig. 1C). This region (especially TM4), by analogy with that in voltage-gated K^+ channels, is believed to be involved in voltage-dependent gating of such channels, although the origin of the voltage dependence prominent in a few TRPs (including TRPC4/5) remains a puzzle [32]. At the same time, a number of other features we analyzed showed significant species-related differences.

First, the permissive action of intracellular Ca^{2+} is lacking in mouse TRPC4s. This fact is probably related to structural differences in one of the CaM-binding domains of these channels. Even more striking are differences in the voltage-gated kinetics, especially considering the conserved TM1-TM6 region. Obviously, an important part of the voltage dependence has to be extrinsic with respect to this region, most likely contained in the more variable C-terminus. It is here where $G\alpha_i$ subunits bind [24], and we found earlier that activated G-proteins not only open muscarinic channels but also regulate their voltage dependence [19]. Species differences in the whole-cell and single-channel current kinetics reveal, for the first time, that there exist two fundamentally different strategies for the P_o increase in TRPC4 along with G-protein activation. In the guinea pig, this is achieved by the generation of relatively infrequent but long openings. In contrast, shorter but more frequent openings underlie the P_o rise in mouse myocytes.

Investigation of the species-dependent differences in ion channel behavior is promising for at least two reasons. First, it is of a theoretical value for better understanding of the structural basis of channel activation and regulation, which relies on exploiting naturally occurring protein differences. Highlighting this point, recent bioinformatics analysis of a large number of annotated TRP channel sequences (2851 in total) in comparison with voltage-gated K_V1-9 channels (3746 sequences) has revealed an evolutionarily conserved gating mechanism for TRPs [36]. Examination of species-related differences in the TRPA1 cold sensitivity has revealed the molecular determinant of these channels pinpointed to a single amino acid residue in the TM5 transmembrane segment (Gly_{878} in cold-sensitive rodent TRPA1 but Val_{875} in cold-insensitive primate TRPA1) [37]. In another study, marked differences in the TRPV2 responses to heating and to a non-selective agonist, 2-APB, were shown to exist between heterologously expressed mouse, rat, or human channels (notably, human TRPV2 was found to be nonresponsive to these activators) [38]. The growing list of such studies within the TRP area has recently been reviewed [32].

Second, it is of considerable practical value for translational research and drug development. For example, blockers of TRPC4 hold promise as an alternative to mAChR blockers (e.g., in asthma, overactive bladder, and IBS), which are efficient but lack the selectivity for mAChR subtypes and, thus, cause strong multiple side effects. Channel blockers fall into two main categories, those occluding the channel pore and the so-called gating modifiers. Here, we showed that different rodent species may use different gating modes to increase P_o. Thus, studies of mI_{CAT} in human tissues are ultimately needed, in order to determine the optimal mechanism of channel blocking in humans. In this relation, it is interesting to note that the guinea-pig and mouse, both belonging to the order Rodentia, have different lineages, namely Rodentia–Hystricognathi–Caviidae–*Cavia* and Rodentia–Sciurognathi–Muroidea–Muridae–Murinae–*Mus*–*Mus*. BLAST analysis showed that the closest counterparts of human TRPC4, besides eight primates that have the highest (99.5–98.8%) structural homology but are rarely used in laboratories, are TRPC4s in the

rabbit (98.7%), dog (98.2%), pig (97.4%), Chinese hamster (97.4%), guinea-pig (97.1%), rat (97,0%), and mouse (96.8%). Interestingly the inward current evoked by mAChR stimulation in the small intestine of the rabbit is generated predominantly via a Ca^{2+}-dependent mechanism rather than via a G-protein one [39].

In conclusion, TRPC4 structural differences between the two rodent species are mainly related to channel regulation by G-proteins, likely via its C-terminus, rather than via its core voltage-dependent properties. The differences we described open new prospects for further structure/function studies of mAChR-operated cation channels in visceral smooth muscles.

Acknowledgments. This study was supported by the Wellcome Trust (grant 062926) and U.S. National Institutes of Health (grant DK081654).

The authors would like to thank Dr. D. A. Vasilenko for helpful discussion of several important aspects of this work.

All experimental procedures were carried out in accordance with guidelines for animal care and use in sientific studies; this was confirmed by the Ethic Commities of the Institute of biology (Taras Shevchenko University) and Bohomolets Institute of physiology of the NAS of Ukraine.

The authors, D. O. Dryn, A. V. Gryshchenko, T. B. Boltan, M. X. Zhu, and A. V. Zholos, confirm that they have no conflicts of any kind related to the commercial or financial problems, relations with organizations or persons, which could in any way be associated with the investigation, and with the relationship of the co-authors of the article.

Д. О. Дринь[1], О. В. Грищенко[2], Т. Б. Болтон[3], М. Кс. Жу[4], О. В. Жолос[1,2]

ВИДОВІ РОЗБІЖНОСТІ ВЛАСТИВОСТЕЙ КАНАЛІВ TRPC4 В МІОЦИТАХ КИШКІВНИКА ГРИЗУНІВ

[1] Освітньо-науковий центр «Інститут біології» національного Університету ім. Тараса Шевченка, Київ (Україна).
[2] Інститут фізіології ім. О. О. Богомольця НАН України, Київ (Україна).
[3] Лондонський університет Святого Георгія (Велика Британія).
[4] Університет Техасу, Центр наук про здоров'я у Х'юстоні, (США).

Р е з ю м е

Протеїни TRPC4 формують рецепторкеровані катіонні канали, які активуються синергічною дією на M_2- та M_3-ацетилхолінові рецептори, відповідно пов'язані з $G_{q/11}$- та $G_{i/o}$-протеїнами. Ці канали широко експресовані в мозку та гладеньких м'язах, де вони виконують численні функції, в тому числі забезпечуючи контроль вивільнення ГАМК із дендритів та холінергічне збудження гладеньких м'язів. Біофізичні властивості струмів через TRPC4-канали, індукованих у клітинах миші прямою дією ГТФγS, залишаються великою мірою невідомими. Тому ми досліджували ці канали в міоцитах тонкого кишківника миші, в яких спостерігається значний катіонний струм, опосередкований TRPC4 та названий mI_{CAT}. Ми порівнювали властивості даного струму з властивостями краще вивченого mI_{CAT} у міоцитах морської свинки. Незважаючи на те що катіонні струми після аплікації карбахолу при потенціалі –50 мВ (тобто при значенні, близькому до нормального потенціалу спокою в цих клітинах) були дуже подібними, вплив внутрішньоклітинного кальцію на відкривання досліджуваних каналів під час відведення mI_{CAT} у миші був відсутнім. Швидкість зміни мускаринової катіонної провідності, котра є визначальним фактором щодо потенціалзалежної поведінки каналів, у двох згаданих видів гризунів була практично ідентичною. Спостерігалися помітні розбіжності значень негативних потенціалів, при яких струм досягав максимуму, але максимальні щільності струмів були подібними. Найбільші відмінності були виявлені в кінетиці потенціалзалежної релаксації mI_{CAT}, котра у миші була значно швидшою. У вказаних видів гризунів використовуються дві відмінні стратегії підвищення вірогідності відкритого стану досліджуваних каналів при активації G-протеїнів. Середнє значення часу відкритого стану у миші було значно меншим порівняно з відповідним показником у морської свинки (15.1 ± 5.2 мс, n = 8, vs 80.0 ± 19.7 мс, n = 9; $P < 0.01$). Відповідно, у миші миттєва частота відкривань каналів була значно вищою, ніж у морської свинки (154.1 ± 18.8 c^{-1} vs 70.2 ± ± 7.3 c^{-1}; $P < 0.001$). Ці функціональні різниці розглядаються як наслідок структурних розбіжностей відповідних послідовностей амінокислотних залишків у білках TRPC4 двох вказаних видів гризунів. Дані розбіжності в основному сконцентровані в цитозольних С-закінченнях первинних послідовностей протеїнів TRPC4.

REFERENCES

1. R. M. Eglen, S. S. Hegde, and N. Watson, "Muscarinic receptor subtypes and smooth muscle function," *Pharmacol. Rev.,* **48,** 531-565 (1996).
2. A. V. Zholos, "Muscarinic effects on ion channels in smooth muscle cells," *Neurophysiology*, **31,** No. 3, 173-187 (1999**)**.
3. K. M. Sanders, "G protein-coupled receptors in gastrointestinal physiology. IV. Neural regulation of gastrointestinal smooth muscle," *Am. J. Physiol.,* **275,** G1-G7 (1998).
4. T. B. Bolton, S. A. Prestwich, A. V. Zholos, and D. V. Gordienko. "Excitation-contraction coupling in gastrointestinal and other smooth muscles," *Annu. Rev. Physiol.,* **61,** 85-115 (1999).
5. H. Kuriyama, K. Kitamura, T. Itoh, and R. Inoue, "Physiological features of visceral smooth muscle cells, with

special reference to receptors and ion channels," *Physiol. Rev.,* **78,** 811-920 (1998).
6. A.V. Zholos, "Regulation of TRP-like muscarinic cation current in gastrointestinal smooth muscle with special reference to PLC/$InsP_3$ /Ca^{2+} system," *Acta Pharmacol. Sin.,* **27,** 833-842 (2006).
7. I. So and K. W. Kim, "Nonselective cation channels activated by the stimulation of muscarinic receptors in mammalian gastric smooth muscle," *J. Smooth Muscle Res.,* **39,** 231-247 (2003).
8. T. B. Bolton, "Mechanisms of action of transmitters and other substances on smooth muscle," *Physiol. Rev.,* **59,** 606-718 (1979).
9. A. V. Zholos, V. V. Tsvilovskyy, and T. B. Bolton, "Muscarinic cholinergic excitation of smooth muscle: signal transduction and single cationic channel properties," *Neurophysiology*, **35**, Nos. 3/4, 283-301 (2003).
10. A. V. Zholos and T. B. Bolton, "Muscarinic receptor subtypes controlling the cationic current in guinea-pig ileal smooth muscle," *Br. J. Pharmacol.,* **122,** 885-893 (1997).
11. H. D. Yan, H. Okamoto, T. Unno, et al., "Effects of G-protein-specific antibodies and Gβγ subunits on the muscarinic receptor-operated cation current in guinea-pig ileal smooth muscle cells," *Br. J. Pharmacol.,* **139,** 605-615 (2003).
12. R. Inoue and G. Isenberg, "Intracellular calcium ions modulate acetylcholine-induced inward current in guinea-pig ileum," *J. Physiol.,* **424,** 73-92 (1990).
13. P. Pacaud and T.B. Bolton, "Relation between muscarinic receptor cationic current and internal calcium in guinea-pig jejunal smooth muscle cells," *J. Physiol.,* **441,** 477-499 (1991).
14. D. V. Gordienko and A. V. Zholos, "Regulation of muscarinic cationic current in myocytes from guinea-pig ileum by intracellular Ca^{2+} release: a central role of inositol 1,4,5-trisphosphate receptors," *Cell Calcium,* **36,** 367-386 (2004).
15. Ya. D. Tsytsyura, A. V. Zholos, M. F. Shuba, and T. B. Bolton, "Effect of intracellular Ca^{2+} on muscarinic cationic current in guinea pig ileal smooth muscle cells," *Neurophysiology,* **32,** No. 3, 198-199 (2000).
16. C. D. Benham, T. B. Bolton, and R. J. Lang, "Acetylcholine activates an inward current in single mammalian smooth muscle cells," *Nature,* **316,** 345-347 (1985).
17. R. Inoue, K. Kitamura, and H. Kuriyama, "Acetylcholine activates single sodium channels in smooth muscle cells," *Pflügers Arch.,* **410,** 69-74 (1987).
18. R. Inoue and G. Isenberg, "Effect of membrane potential on acetylcholine-induced inward current in guinea-pig ileum," *J. Physiol.,* **424,** 57-71 (1990).
19. A. V. Zholos and T. B. Bolton, "G-protein control of voltage dependence as well as gating of muscarinic metabotropic channels in guinea-pig ileum," *J. Physiol.,* **478,** 195-202 (1994).
20. A. V. Dresviannikov, T. B. Bolton, and A. V. Zholos, "Muscarinic receptor-activated cationic channels in murine ileal myocytes," *Br. J. Pharmacol.,* **149,** 179-187 (2006).
21. T. Sakamoto, T. Unno, T. Kitazawa, et al., "Three distinct muscarinic signalling pathways for cationic channel activation in mouse gut smooth muscle cells," *J. Physiol.,* **582,** 41-61 (2007).
22. V. V. Tsvilovskyy, A. V. Zholos, T. Aberle, et al., "Deletion of TRPC4 and TRPC6 in mice impairs smooth muscle contraction and intestinal motility *in vivo,*" *Gastroenterology,* **137,** 1415-1424 (2009).
23. K. P. Lee, J. Y. Jun, I. Y. Chang, et al., "TRPC4 is an essential component of the nonselective cation channel activated by muscarinic stimulation in mouse visceral smooth muscle cells," *Mol. Cells,* **20,** 435-441 (2005).
24. J. P. Jeon, C. Hong, E. J. Park, et al., "Selective $G\alpha_i$ subunits as novel direct activators of transient receptor potential canonical TRPC4 and TRPC5 channels," *J. Biol. Chem.,* **287,** 17029-17039 (2012).
25. K. Otsuguro, J. Tang, Y. Tang, et al., "Isoform-specific inhibition of TRPC4 channel by phosphatidylinositol 4,5-bisphosphate," *J. Biol. Chem.,* **283,** 10026-10036 (2008).
26. M. X. Zhu, "Multiple roles of calmodulin and other Ca^{2+}-binding proteins in the functional regulation of TRP channels," *Pflugers Arch.,* **451,** 105-115 (2005).
27. K. Venkatachalam and C. Montell, "TRP channels," *Annu. Rev. Biochem.,* **76,** 387-417 (2007).
28. A. V. Zholos, A. A. Zholos, and T. B. Bolton, "G-protein-gated TRP-like cationic channel activated by muscarinic receptors: effect of potential on single-channel gating," *J. Gen. Physiol.,* **123,** 581-598 (2004).
29. I. C. Spyropoulos, T. D. Liakopoulos, P. G. Bagos, and S. J. Hamodrakas, "TMRPres2D: high quality visual representation of transmembrane protein models". *Bioinformatics,* **20,** 3258-3260 (2004).
30. J. Soding, "Protein homology detection by HMM-HMM comparison," *Bioinformatics,* **21,** 951-960 (2005).
31. M. A. Larkin, G. Blackshields, N. P. Brown, et al., "Clustal W and Clustal X version 2.0." *Bioinformatics,* **23,** 2947-2948 (2007).
32. B. Nilius and V. Flockerzi, "What do we really know and what do we need to know: some controversies, perspectives, and surprises," *Handbook Exp. Pharmacol.,* **223**, 1239-1280 (2014).
33. M. Freichel, V. Tsvilovskyy, and J. E. Camacho-Londono, "TRPC4- and TRPC4-containing channels," *Handbook Exp. Pharmacol.,* **222**, 85-128 (2014).
34. J. Tang, Y. Lin, Z. Zhang, et al., "Identification of common binding sites for calmodulin and inositol 1,4,5-trisphosphate receptors on the carboxyl termini of Trp channels," *J. Biol. Chem.,* **276,** 21303-21310 (2001).
35. A.V. Zholos and T.B. Bolton, "A novel GTP-dependent mechanism of ileal muscarinic metabotropic channel desensitization," *Br. J. Pharmacol.,* **119,** 997-1012 (1996).
36. E. Palovcak, L. Delemotte, M. L. Klein, and V. Carnevale, "Comparative sequence analysis suggests a conserved gating mechanism for TRP channels," *J. Gen. Physiol.,* **146,** 37-50 (2015).
37. J. Chen, D. Kang, J. Xu, et al., "Species differences and molecular determinant of TRPA1 cold sensitivity," *Nat. Commun.,* **4**, 2501 (2013).
38. M. P. Neeper, Y. Liu, T. L. Hutchinson, et al., "Activation properties of heterologously expressed mammalian TRPV2: Evidence for species dependence," *J. Biol. Chem.,* **282,** 15894-15902 (2007).
39. S. P. Lim and T. B. Bolton, "A calcium-dependent rather than a G-protein mechanism is involved in the inward current evoked by muscarinic receptor stimulation in dialysed single smooth muscle cells of small intestine," *Br. J. Pharmacol.,* **95,** 325-327 (1988).